Journal of Structural Geology, Vol. 12, No. 8, pp. 1067 to 1071, 1990
Printed in Great Britain

0191-8141/90 $03.00+0.00

Critical stress difference and orientation of faults in rocks with strength anisotropies: the two-dimensional case

G. RANALLI and Z.-M. YIN

Department of Earth Sciences and Ottawa-Carleton Geoscience Centre, Carleton University, Ottawa, Canada K1S 5B6

(*Received* 11 *December* 1989; *accepted in revised form* 1 *May* 1990)

Abstract—Equations are derived for the critical stress difference on thrust, normal and strike-slip faults with finite cohesive strength, both in homogeneous, isotropic rock, and along pre-existing strength anisotropies with different cohesion and coefficient of friction, subject to the limitation that the plane of anisotropy contains the intermediate axis of stress. The range of orientations for which sliding occurs along pre-existing planes of weakness rather than along a new fault is given as a function of material parameters and critical stress difference for the intact rock. Given the principal stress directions, the equations allow the direct calculation of the stress and orientation conditions for the three faulting regimes.

INTRODUCTION

BRITTLE shear failure in the upper lithosphere is usually described in terms of the Coulomb–Navier fracture criterion. On the assumption that this criterion adequately describes faulting, it is possible to predict the orientation of fracture planes and the critical state of stress (see e.g. Jaeger & Cook 1969, Ranalli 1987, Mandl 1988). Assuming vertical orientation of one principal stress, Anderson (1905, 1951) provided a model for normal, strike-slip and thrust faulting. Sibson (1974) derived expressions for the critical stress difference in the three faulting regimes on planes most favourably oriented for faulting and with negligible cohesive strength.

In this paper, we extend Sibson's analysis to include fracture planes with finite cohesive strength and arbitrary orientation with respect to the maximum stress axis. Fundamental to our analysis is the concept of strength anisotropy, i.e. a plane within the rock along which cohesive strength and/or coefficient of friction are less than the corresponding quantities in intact, isotropic rock. Strength anisotropies may be introduced by the presence of pre-existing fracture planes, layering, fabric, etc. Although similar problems have been considered before (e.g. Jaeger 1960, Jaeger & Cook 1969, Sibson 1985, Nur *et al.* 1986; see summary by Ivins *et al.* 1990), to our knowledge no unified quantitative treatment in terms of the three tectonic faulting regimes is available. The present analysis is limited to the case when the plane of anisotropy contains the intermediate stress axis; relaxation of this condition introduces further complexities and is at present under investigation.

CRITICAL STRESS DIFFERENCE ON MOST FAVOURABLY ORIENTED FAULTS

The Coulomb–Navier shear failure criterion is

$$\tau = S + \mu\sigma, \qquad (1)$$

where τ, σ are shear and normal stress on the fracture plane, and S, μ are cohesive strength and coefficient of friction (denoted as S_0, μ_0 if referring to a strength anisotropy). As the occurrence of fracture depends only on the magnitude of the shear stress, we restrict our attention to positive values. Compression is taken as positive.

Sibson (1974) derived expressions for the critical stress difference on cohesionless ($S_0 = 0$) pre-existing fracture planes most favourably oriented (that is, making an angle $\theta = \frac{1}{2}\tan^{-1}(1/\mu_0)$) with the axis of maximum compression. If $\sigma_1 > \sigma_2 > \sigma_3$ are the principal stresses, $R = \sigma_1/\sigma_3$ the principal stress ratio, z depth, $\mathbf{g}$ gravity, ρ the average density of overlying rock, and λ the pore-fluid factor (ratio of pore-fluid pressure to overburden pressure), the general conditions for sliding on thrust, normal and strike-slip faults are, respectively,

$$(\sigma_1 - \sigma_3) = (R-1)\rho \mathbf{g} z(1-\lambda) \qquad (2a)$$

$$(\sigma_1 - \sigma_3) = \frac{R-1}{R}\rho \mathbf{g} z(1-\lambda) \qquad (2b)$$

$$(\sigma_1 - \sigma_3) = \frac{R-1}{1+\delta(R-1)}\rho \mathbf{g} z(1-\lambda). \qquad (2c)$$

frictional properties as

$$R = [(\mu_0^2+1)^{1/2} + \mu_0]^2. \qquad (3)$$

The factor δ ($0 < \delta < 1$) appearing in equation (2c) comes from writing the intermediate principal stress as $\sigma_2 = \sigma_3 + \delta(\sigma_1 - \sigma_3)$. The critical stress difference is larger for thrust faults than for strike-slip and normal faults (in that order).

The assumption $S_0 = 0$ restricts the applicability of equations (2) to cohesionless pre-existing fracture planes. The analysis, however, can be readily extended to new faults in homogeneous, isotropic rock, for which $S > S_0$ and $\mu \neq \mu_0$. Considering the expressions for shear and normal stresses on a plane containing the σ_2-axis and

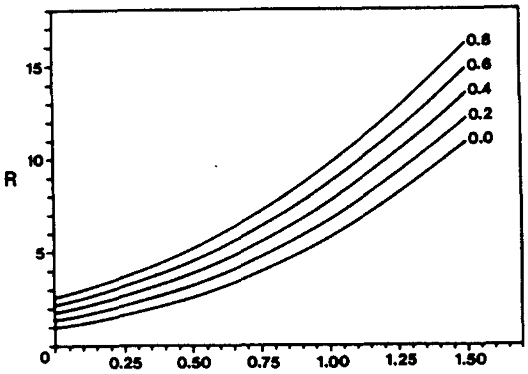

Fig. 1. Principal stress ratio $R = \sigma_1/\sigma_3$ at failure as a function of the friction coefficient, μ. Numbers on curves denote values of S/σ_3.

making an angle θ with the σ_1-axis (see e.g. Jaeger & Cook 1969, pp. 87–91), the Coulomb–Navier criterion can be written as

$$S + \mu\left[\tfrac{1}{2}(\sigma_1 + \sigma_3) - \tfrac{1}{2}(\sigma_1 - \sigma_3)\cos 2\theta\right] = \tfrac{1}{2}(\sigma_1 - \sigma_3)\sin 2\theta \tag{4}$$

which, in terms of the principal stress ratio R, becomes

$$2\frac{S}{\sigma_3} + \mu[(R + 1) - (R - 1)\cos 2\theta] = (R - 1)\sin 2\theta. \tag{5}$$

Equation (5), together with the condition that the critical angle is $\theta = \frac{1}{2}\tan^{-1}(1/\mu)$ which can be derived from equation (4), yields an expression for the principal stress ratio

$$R = 2\frac{S}{\sigma_3}[(\mu^2 + 1)^{1/2} + \mu] + [(\mu^2 + 1)^{1/2} + \mu]^2 \tag{6}$$

that reduces to equation (3) (Sibson 1974) for $S = 0$, $\mu = \mu_0$.

The variation of R with the coefficient of friction for various values of the ratio between cohesive strength and minimum principal stress is shown in Fig. 1. The critical stress differences for thrust, normal and strike-slip faulting along new fracture planes are formally identical to equations (2), with R given by equation (6) rather than (3). The critical stress ratio can be written as a function of material parameters and overburden pressure by eliminating σ_3 in equation (6). In the case of thrust faulting, where $\sigma_3 = \rho g z(1 - \lambda)$, it becomes

$$R = \frac{2S}{\rho g z(1-\lambda)}[(\mu^2+1)^{1/2}+\mu]+[(\mu^2+1)^{1/2}+\mu]^2. \tag{7a}$$

In the case of normal faulting, where $\sigma_3 = \rho g z(1 - \lambda)/R$,

$$R = \frac{[(\mu^2 + 1)^{1/2} + \mu]^2 \rho g z(1 - \lambda)}{\rho g z(1 - \lambda) - 2S[(\mu^2 + 1)^{1/2} + \mu]}. \tag{7b}$$

In the case of strike-slip faulting, where $\sigma_3 = \rho g z(1 - \lambda)/[1 + \delta(R - 1)]$,

$$R = \frac{2(1 - \delta)S[(\mu^2 + 1)^{1/2} + \mu] + [(\mu^2 + 1)^{1/2} + \mu]^2 \rho g z(1 - \lambda)}{\rho g z(1 - \lambda) - 2S\delta[(\mu^2 + 1)^{1/2} + \mu]}. \tag{7c}$$

Equations (7) reduce to equation (3) for a cohesionless pre-existing fault. Together with equations (2), they give the critical stress difference for the three faulting regimes in isotropic, intact rock. Finite cohesion has the effect of making R depth-dependent, which is not the case for cohesionless material. For normal and strike-slip faulting, $\sigma_3 < 0$ at shallow depth ($z \le 4S/[\rho g(1 - \lambda)]$ and $z \le 2S/[\rho g(1 - \lambda)]$, respectively, for $\mu = 0.75$ and $\delta = \frac{1}{2}$). Due to cohesion, the critical stress difference at such depths can be reached only if the minimum stress is tensile, and the Coulomb–Navier criterion effectively breaks down. This point is discussed further in the next section.

The critical stress difference $(\sigma_1 - \sigma_3)_N$ along a new fault in homogeneous, isotropic rock with parameters S and μ can be written as a function of the critical stress difference $(\sigma_1 - \sigma_3)_0$ along a most favourably oriented strength anisotropy with parameters S_0 and μ_0, by comparing equation (6) in the two cases and solving for the vertical stress. After some algebra, we obtain for thrust, normal and strike-slip faults, respectively,

$$(\sigma_1 - \sigma_3)_N = (\sigma_1 - \sigma_3)_0\mu' + 2\mu[(\mu^2 + 1)^{1/2} + \mu] \times\left[\frac{S}{\mu} - \frac{S_0}{\mu_0}\right] \tag{8a}$$

$$(\sigma_1 - \sigma_3)_N = (\sigma_1 - \sigma_3)_0\mu'' + 2\mu[(\mu^2 + 1)^{1/2} - \mu] \times\left[\frac{S}{\mu} - \frac{S_0}{\mu_0}\right] \tag{8b}$$

$$(\sigma_1 - \sigma_3)_N = (\sigma_1 - \sigma_3)_0\mu'\mu''' + \frac{2\mu[(\mu^2 + 1)^{1/2} + \mu]}{1 + 2\delta\mu[(\mu^2 + 1)^{1/2} + \mu_0]} \times\left[\frac{S}{\mu} - \frac{S_0}{\mu_0}\right], \tag{8c}$$

where

$$\mu' = \frac{\mu[(\mu^2 + 1)^{1/2} + \mu]}{\mu_0[(\mu_0^2 + 1)^{1/2} + \mu_0]},$$

$$\mu'' = \frac{\mu[(\mu^2 + 1)^{1/2} - \mu]}{\mu_0[(\mu_0^2 + 1)^{1/2} - \mu_1]},$$

$$\mu''' = \frac{1 + 2\delta\mu_0[(\mu_0^2 + 1)^{1/2} + \mu_0]}{1 + 2\delta\mu[(\mu^2 + 1)^{1/2} + \mu]}.$$

The Mohr circles corresponding to these stress states are given in Fig. 2 for the case $S_0 = 0$, $\mu = \mu_0$. The critical stress differences as a function of depth are shown in Fig. 3 for $S = 75$ MPa, $S_0 = 5$ MPa, $\mu_0 = 0.75$, $\delta = \frac{1}{2}$, and two different pore-fluid pressures, corresponding to dry rock ($\lambda = 0$) and to approximately hydrostatic ($\lambda = 0.4$) water pressure. The critical stress difference for faulting along new planes in homogeneous, isotropic rock is larger than the stress difference for faulting along most favourably oriented strength anisotropies, by an amount (constant in the particular case $\mu = \mu_0$) which depends on material parameters and faulting regime.

CRITICAL STRESS DIFFERENCE AND CRITICAL ANGLE FOR STRENGTH ANISOTROPIES

The critical stress difference for strength anisotropies oriented most favourably for fracture is less than that for new fracture planes in isotropic rock. When a strength anisotropy is oriented at a different angle γ with respect to the axis of maximum compression ($\gamma \neq \theta = \frac{1}{2}\tan^{-1}(1/\mu)$), the critical stress difference is larger than that for the most favourably oriented anisotropy; however, depending on orientation, it may still be less than the critical stress difference for failure in isotropic rock. We first give the critical stress difference for an anisotropy containing the σ_2-axis and making an arbitrary angle γ with the σ_1-axis as a function of material parameters and orientation; we then derive expressions defining the range of orientations for which sliding occurs on pre-existing strength anisotropies rather than on newly formed planes of fracture. Although both problems have been considered before (see e.g. Jaeger & Cook 1969, Sibson 1985, Nur *et al.* 1986), we give new explicit equations for critical stress differences and orientations for each faulting regime.

In the following, $(\sigma_1 - \sigma_3)_A$ and $(\sigma_1 - \sigma_3)_N$ are the critical stress differences for an arbitrarily oriented anisotropy containing the σ_2-axis and a new plane of fracture, with parameters S_0, μ_0, S and μ, respectively. In a thrust faulting regime, where the vertical stress is σ_3, equation (4) can be solved for σ_3 in both cases. By equating the two solutions we obtain

$$(\sigma_1-\sigma_3)_A = \frac{(\sigma_1-\sigma_3)_N\mu_0[(\mu^2+1)^{1/2}-\mu]+2(S_0\mu-S\mu_0)}{\mu[\sin 2\gamma+\mu_0(\cos 2\gamma-1)]}. \tag{9a}$$

In a normal faulting regime, where the vertical stress is σ_1, the same procedure and solving for σ_1 yields

$$(\sigma_1-\sigma_3)_A = \frac{(\sigma_1-\sigma_3)_N\mu_0[(\mu^2+1)^{1/2}+\mu]+2(S_0\mu-S\mu_0)}{\mu[\sin 2\gamma+\mu_0(\cos 2\gamma+1)]}. \tag{9b}$$

In a strike-slip faulting regime, where the vertical stress is $\sigma_2 = \sigma_3 + \delta(\sigma_1 - \sigma_3)$, we obtain

$$(\sigma_1-\sigma_3)_A = \frac{(\sigma_1-\sigma_3)_N\mu_0[(\mu^2+1)^{1/2} -\mu+2\mu\delta]+2(S_0\mu-S\mu_0)}{\mu[\sin 2\gamma+\mu_0(\cos 2\gamma-1+2\delta)]}. \tag{9c}$$

Equations (9) reduce to the criterion for sliding on a most favourably oriented pre-existing fault for $\gamma = \theta$. Critical stress differences in the thrust regime for strength anisotropies of various orientations are compared in Fig. 4 with critical stress differences for the formation of a new fault and for slippage along a most favourably oriented anisotropy.

For a given stress regime, failure along a strength anisotropy occurs only as long as the critical shear stress is less than that for the formation of a new fault cutting the anisotropy. The orientation conditions for faulting along a strength anisotropy are shown in Fig. 5. The angles α and β define the limits within which sliding occurs along the anisotropy. Outside this range, a new fault forms with orientation $\theta = \frac{1}{2}\tan^{-1}(1/\mu)$. Expressions for the limiting angles for the three types of faulting can be obtained from equation (4), solving it twice for $(\sigma_1 + \sigma_3)$, once in terms of S, μ and θ, and once in terms of S_0, μ_0 and γ. Equating the two solutions and introducing the angle of internal friction $\phi_0 = \tan^{-1}(\mu_0)$, we have

$$\alpha = \frac{1}{2}\left\{\sin^{-1}\left[\frac{\mu_0(\sigma_1-\sigma_3)_N(\mu^2+1)^{1/2} + 2(S_0\mu - S\mu_0)}{\mu(\sigma_1-\sigma_3)_N(\mu_0^2+1)^{1/2}}\right] - \phi_0\right\} \tag{10a}$$

$$\beta = \frac{\pi}{2} - \frac{1}{2}\left\{\sin^{-1}\left[\frac{\mu_0(\sigma_1-\sigma_3)_N(\mu^2+1)^{1/2} + 2(S_0\mu - S\mu_0)}{\mu(\sigma_1-\sigma_3)_N(\mu_0^2+1)^{1/2}}\right] + \phi_0\right\} \tag{10b}$$

for the minimum and maximum limiting angle, respectively.

Equations (10) give the range of favourable orientations of strength anisotropies (with respect to the maximum stress axis) as a function of material parameters and of critical stress difference. Although material parameters are assumed not to depend on depth, critical angles do, as the critical stress difference is a function of depth. They also depend on fault type. Figure 6 gives α and β as a function of depth and faulting regime for two representative values of pore-fluid pressure. The orientation range for which sliding occurs along pre-existing planes of weakness decreases in going from normal to thrust faults at any depth. For any given faulting regime and pore-fluid pressure, the orientation range decreases with increasing depth. The results of this analysis can be compared with the particular case of reactivation of pre-existing cohesionless faults (Sibson 1985). The three-dimensional case for extensional reac-

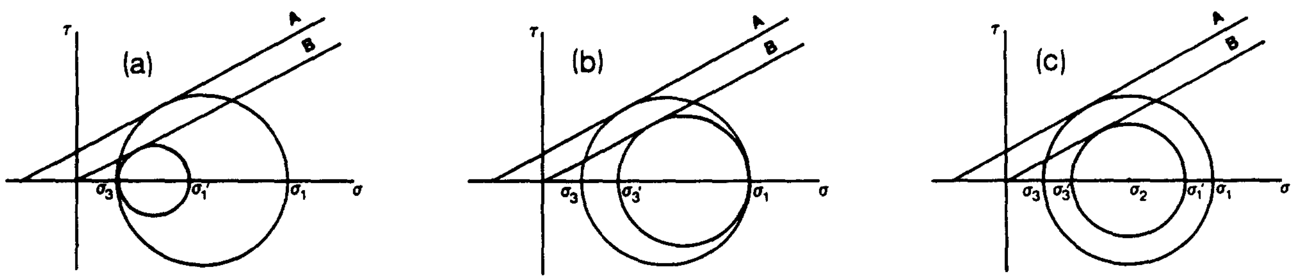

Fig. 2. Mohr circles and failure envelopes (denoted by A and B for finite cohesion and cohesionless pre-existing fault, respectively) in the case of (a) thrust faulting, (b) normal faulting and (c) strike-slip faulting, assuming $\mu = \mu_0$ and $\delta = \frac{1}{2}$. In all three cases, the principal vertical stress does not change, but failure along the pre-existing fault occurs at a lower critical stress difference (primes denote critical stresses for pre-existing faults).

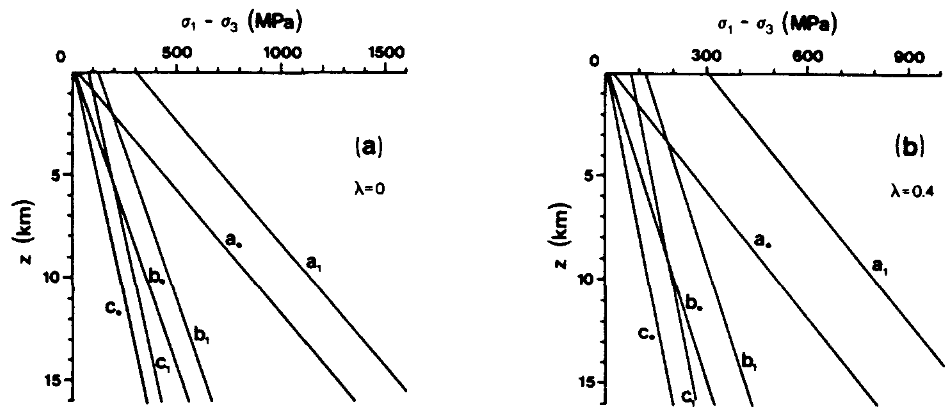

Fig. 3. Critical stress difference ($\sigma_1 - \sigma_3$) vs depth (z) for homogeneous, isotropic rock (a_1, b_1, c_1) and for most favourably oriented anisotropies (a_0, b_0, c_0) in thrust, strike-slip and normal faulting regimes, respectively. Two cases are presented: (a) no pore fluid pressure; and (b) ratio of pore fluid to overburden pressure $\lambda = 0.4$. Parameters are $S = 75$ MPa, $S_0 =$ 5 MPa, $\mu = \mu_0 = 0.75$, $\delta = \frac{1}{2}$ and $\rho = 2700$ kg m^{-3}.

tivation of pre-existing thrust faults has been treated by Ivins *et al.* (1990): their limiting angle can be proven to be equivalent to that given by equation (10b) for normal faulting (Ivins personal communication 1990).

At shallow depths, α can be negative for normal and strike-slip faults: consequently, the Coulomb–Navier criterion is not formally valid and σ_3 must be tensional. The depth range for which this is the case is determined by the range in which $R < 0$ (see previous section), and is a function of cohesion and pore fluid pressure. For low cohesion (5 MPa), it is only a few hundred metres; for high cohesion (75 MPa, which is probably an upper limit) it is about 5 and 10 km for strike-slip and normal faults, respectively, in the absence of pore fluid pressure. Physically, the need for tensional minimum stress in normal and strike-slip faulting arises from the fact that, since the overburden pressure (σ_1 for normal faulting, σ_2 for strike-slip faulting) is low at shallow depths, the critical stress difference $\sigma_1 - \sigma_3$ becomes sufficiently large only for $\sigma_3 < 0$. This limitation does not apply to thrust faulting, where the overburden pressure is σ_3. In practice, dynamic conditions at fault tips may allow a normal or a strike-slip fault to propagate to the surface under compression, but such faults probably originate below the critical depth.

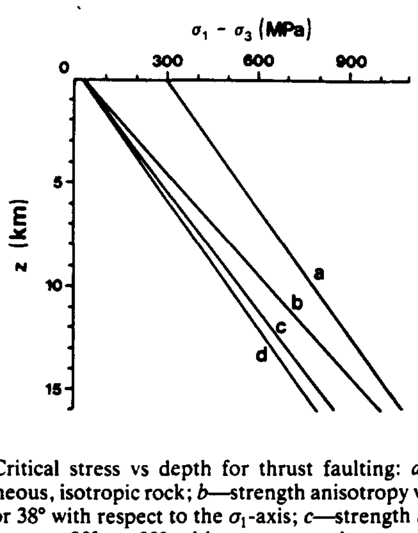

Fig. 4. Critical stress vs depth for thrust faulting: a—new fault in homogeneous, isotropic rock; b—strength anisotropy with orientation $\gamma = 15°$ or $38°$ with respect to the σ_1-axis; c—strength anisotropy with orientation $\gamma = 20°$ or $33°$ with respect to the σ_1-axis; d—strength anisotropy with orientation $\gamma = \theta = \frac{1}{2}\tan^{-1}(1/\mu_0)$. Material parameters as for Fig. 3, with $\lambda = 0.4$. The two values of γ in each case are symmetric with respect to the critical angle θ.

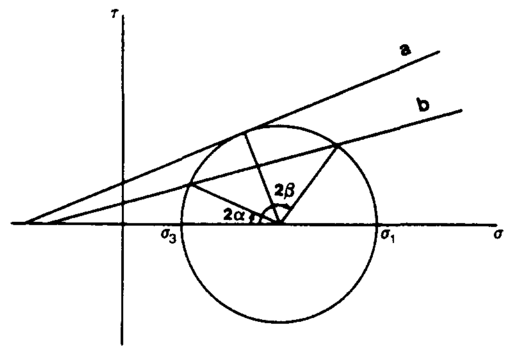

Fig. 5. Mohr circle for failure in homogeneous, isotropic rock and along strength anisotropy (a and b, respectively). Failure occurs along the strength anisotropy for orientations $\alpha \leq \gamma \leq \beta$ with respect to the axis of maximum compression.

DISCUSSION

The results given in this note are valid for strength anisotropies containing the σ_2-axis (which is either horizontal or vertical, depending on the faulting regime) and can be summarized as follows.

(1) Sibson's (1974) equations for the critical stress difference for sliding on most favourably oriented thrust, normal and strike-slip faults have been extended to the case of finite cohesion; e.g. to the formation of new faults (equations 2 and 7). The critical stress difference in homogeneous, isotropic rock relative to that along a strength anisotropy has been expressed in terms of material parameters (equations 8).

(2) Relations between the critical stress difference along an arbitrarily oriented strength anisotropy and that for a homogeneous, isotropic rock have been obtained for the three faulting regimes, in terms of material parameters and orientation (equations 9).

(3) The range of orientations for which sliding occurs along a pre-existing plane of weakness rather than along a newly formed fault has been derived as a function of

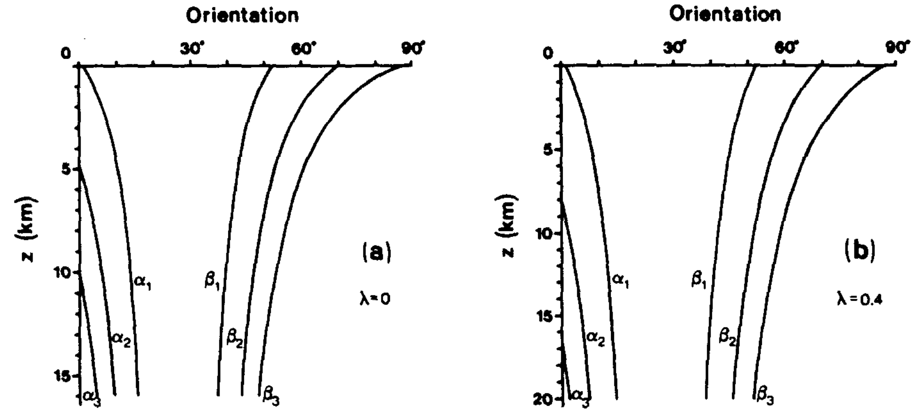

Fig. 6. Critical angles α and β for failure along pre-existing anisotropies vs depth for thrust (α_1, β_1), strike-slip (α_2, β_2) and normal faulting (α_3, β_3), in the case of (a) no pore fluid pressure and (b) ratio of pore fluid pressure to overburden pressure $\lambda = 0.4$. Material parameters as for Fig. 3.

material parameters and the critical stress difference in homogeneous, isotropic rock (equations 10).

Although the discussion of detailed case histories is beyond the scope of the work reported here, it is worth pointing out that, given the complex geometry of faults and fault systems (see e.g. Ranalli 1980, Okubo & Aki 1987, Walsh & Watterson 1988, among others) and the presence of strength anisotropies at all scales, the relation between tectonic stress field and fault orientation must be interpreted with care. For instance, low-angle normal faults under certain conditions may be reactivated thrusts in an Andersonian extensional regime, although they may of course be the result of new fracturing in more complex stress fields (Yin 1989). Also, it is commonly assumed in seismicity studies that seismic risk along different segments of a large fault depends in part on variations of frictional and cohesive properties along the fault. While this is certainly valid in well-documented cases, it is highly likely that variations in fault orientation also play an important role, since the critical stress difference required for sliding depends on the orientation of the fracture plane with respect to the stress field (see Tajima & Célérier 1989 for an example of three-dimensional seismological analysis of fault reactivation).

The present approach has two major limitations: it is essentially two-dimensional (which constrains both the fault plane and the plane of anisotropy to contain the intermediate stress direction), and it assumes an Andersonian stress system (one principal stress direction vertical). It nevertheless represents a systematic generalization of the two-dimensional shear failure criterion as applied to geological faulting. Work is in progress to extend it to the three-dimensional case.

Acknowledgements—Comments by various readers of earlier drafts and suggestions by two referees (E. R. Ivins and R. H. Sibson) have been very helpful in the preparation of this paper. E. R. Ivins is thanked for a preprint. Sheila Thayer and Lise Bender assisted with word-processing and drafting. Support was provided by a grant (to G. Ranalli) from the Natural Sciences and Engineering Research Council of Canada.

REFERENCES

Anderson, E. M. 1905. The dynamics of faulting. *Trans. Geol. Soc. Edin.* **8**, 393–402.

Anderson, E. M. 1951. *The Dynamics of Faulting and Dyke Formation* (2nd edn). Oliver & Boyd, Edinburgh.

Ivins, E. R., Dixon, T. H. & Golombek, M. P. 1990. Extensional reactivation of an abandoned thrust: a bound on shallowing in the brittle regime. *J. Struct. Geol.* **12**, 303–314.

Jaeger, J. C. 1960. Shear fracture of anisotropic rocks. *Geol. Mag.* **97**, 65–72.

Jaeger, J. C. & Cook, N. G. W. 1969. *Fundamentals of Rock Mechanics* (3rd edn). Chapman & Hall, London.

Mandl, G. 1988. *Mechanics of Tectonic Faulting*. Elsevier, Amsterdam.

Nur, A., Ron, H. & Scotti, O. 1986. Fault mechanics and the kinematics of block rotations. *Geology* **14**, 746–749.

Okubo, P. & Aki, K. 1987. Fractal geometry in the San Andreas fault system. *J. geophys. Res.* **92**, 345–355.

Ranalli, G. 1980. A stochastic model for strike-slip faulting. *Math. Geol.* **12**, 399–412.

Ranalli, G. 1987. *Rheology of the Earth*. Allen & Unwin, London.

Sibson, R. H. 1974. Frictional constraints on thrust, wrench, and normal faults. *Nature* **249**, 542–544.

Sibson, R. H. 1985. A note on fault reactivation. *J. Struct. Geol.* **7**, 751–754.

Tajima, F. & Célérier, B. 1989. Possible focal mechanism change during reactivation of a previously ruptured subduction zone and stress tensor implications. *Geophys. J. Int.* **98**, 301–316.

Walsh, J. J. & Watterson, J. 1988. Analysis of the relationship between displacements and dimensions of faults. *J. Struct. Geol.* **10**, 239–247.

Yin, A. 1989. Origin of regional, rooted low-angle normal faults: a mechanical model and its tectonic implications. *Tectonics* **8**, 469–482.